Inorg. Chem. **2004**, *43*, 8085–8091

Hydrothermal Syntheses, Crystal Structures, and Properties of a Novel Class of 3,3′,4,4′-Benzophenone-tetracarboxylate (BPTC) Polymers

Jian Zhang, Zhao-Ji Li, Yao Kang, Jian-Kai Cheng, and Yuan-Gen Yao*

State Key Laboratory of Structural Chemistry, Fujian Institute of Research on the Structure of Matter, The Chinese Academy of Sciences, Fuzhou, Fujian 350002, People's Republic of China

Received July 8, 2004

Three novel BPTC complexes, $(H_2BPTC)(4,4'\text{-}H_2bpy)H_2O$ (**1**), $[Cd_2Cu(HBPTC)_2(\mu_2\text{-}4,4'\text{-}bpy)_2(4,4'\text{-}bpy)_2(H_2O)_2]_n$ (**2**), and $[Co_3(HBPTC)_2(\mu_2\text{-}4,4'\text{-}bpy)_3(H_2O)_4]_n{\cdot}2nH_2O$ (**3**) (BPTC = 3,3′,4,4′-benzophenone-tetracarboxylate and bpy = bipyridine), were hydrothermally synthesized. Complex **1**, which is obtained as a coproduct during the syntheses of complexes **2** and **3,** features a 2-D layered strong hydrogen bonding network with 2-fold interpenetration. Complex **2** has an unusual 2-D double-layered motif, which is linked together by Cu atoms in a face-to-face manner. It exhibits nanosized channels filled by 4,4′-bpy ligands. Three six-coordinated Co atoms in **3** are interlinked by HBPTC ligands to form a 2-D grid structure, which is further sustained by rigid 4,4′-bpy ligands into a 3-D open framework similar to $CdSO_4$ with the BPTC moieties situated in the tunnels. The thermal stabilities of complexes **1**–**3** were examined. The photoluminescence properties of complexes **1**–**2** and temperature-dependent magnetic susceptibility for **3** were also studied.

Introduction

Crystal engineering has grown into a subject that attracts intense attention because controlling the molecular organization in the solid state can lead to materials with novel structure and promising properties.[1] Many efforts in this field have focused on the predictable assembly of organic molecular solids and metal coordination compounds (coordination).[2] In this context, there have been major advances with organic−inorganic hybrid systems, and a lot of infinite one-, two-, and three-dimensional metal−organic hybrid compounds synthesized from various metal−ligand building blocks have been reported. In general, structural motifs of these hybrid compounds are closely related to the geometry and the number of coordination sites provided by organic ligands.[3] As an important family of multidentate O-donor ligands, organic aromatic polycarboxylate ligands, such as 1,2-benzenedicarboxylate, 1,3,5-benzenetricarboxylate, and 1,2,4,5-benzenetetracarboxylate, have been extensively employed in the preparation of such metal−organic complexes in possession of multidimensional networks and interesting properties.[4] In this aspect, the 3,3′,4,4′-benzophenonetetracarboxylate (BPTC) ligand (Chart 1), which has nine potential donor oxygen atoms, is a quite versatile ligand for the construction of novel metal−organic hybrid compounds

Chart 1

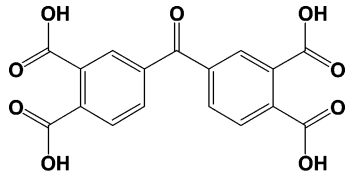

H_4BPTC

* To whom correspondence should be addressed. E-mail: yyg@fjirsm.ac.cn.

(1) (a) Braga, D. *Chem. Commun.* **2003**, 2751. (b) Braga, D.; Desiraju, G. R.; Miller, J. S.; Orpen, A. G.; Price, S. L. *CrystEngComm* **2002**, *4*, 500. (c) Desiraju, G. R. *Crystal Engineering: The Design of Organic Solids*; Elsevier: Amsterdam, 1989. (d) Seddon, K. R.; Zaworotko, M. J. *Crystal Engineering: The Design and Applications of Functional Solids*; NATO ASI Series; Kluwer: Dordecht, 1999. (e) Braga, D.; Orpen, A. G. *Crystal Engineering: From Molecules and Crystals To Materials*; NATO ASI Series; Kluwer: Dordecht, The Netherlands, 1999. (f) Desiraju, G. R. *Crystal Design: Structure and Function, Perspectives in Supramolecular Chemistry*; Wiley: Chichester, 2003; Vol. 6.

(2) (a) Biradha, K. *CrystEngComm* **2003**, *5*, 374. (b) Janiak, C. *J. Chem. Soc., Dalton Trans.* **2003**, 2781. (c) James, S. L. *Chem. Soc. Rev.* **2003**, *32*, 276. (d) Aakeröy, C. B.; Beatty, A. M. In *Comprehensive Coordination Chemistry II*; Elsevier Pergamon: Amsterdam, 2004; Vol. 1, p 679.

(3) (a) Yaghi, O. M.; Li, H.; David, C.; Richardson, D.; Groy, T. L. *Acc. Chem. Res.* **1998**, *31*, 474. (b) Evans, O. R.; Lin, W. *Acc. Chem. Res.* **2002**, *35*, 511. (c) Moulton, B.; Zaworotko, M. J. *Chem. Rev.* **2001**, *101*, 1629.

(4) (a) Li, H.; Eddaoudi, M.; O'Keeffe, M.; Yaghi, O. M. *Nature* **1999**, *402*, 276. (b) Chui, S. S.-Y.; Lo, S. M.-F.; Charmant, J. P. H.; Orpen, A. G.; Williams, I. D. *Science* **1999**, *283*, 1148.

10.1021/ic0491074 CCC: $27.50
Published on Web 11/17/2004

Table 1. Crystallographic Data for the Three Complexes

	1	2	3
empirical formula	$C_{27}H_{20}N_2O_{10}$	$C_{74}H_{50}Cd_2$-CuN_8O_{20}	$C_{64}H_{50}Co_3$-N_6O_{24}
temp (K)	293(2)	293(2)	293(2)
cryst color	yellow	blue	red
cryst size (mm^3)	0.30 × 0.12 ×0.11	0.20 × 0.15 ×0.08	0.55 × 0.15 ×0.07
fw	532.45	1657.54	1463.89
cryst syst	monoclinic	triclinic	monoclinic
space group	$P2_1/c$	$P\bar{1}$	$P2/c$
a (Å)	11.9357(12)	7.52480(10)	11.32(2)
b (Å)	13.5389(13)	10.8479(3)	11.410(5)
c (Å)	14.4089(16)	20.2178(5)	22.795(18)
α (deg)	90	79.0110(10)	90
β (deg)	96.835(2)	87.8000(10)	92.951(14)
γ (deg)	90	80.9930(10)	90
V ($Å^3$)	2311.9(4)	1600.04(6)	2940(6)
Z	4	1	2
density (calcd)	1.530	1.720	1.654
abs coeff (mm^{-1})	0.119	1.077	0.932
F(000)	1104	833	1498
reflns collections	7098	8118	22242
indep reflns	4055[R(int) = 0.0471]	5479[R(int) = 0.0266]	6723[R(int) = 0.0390]
obsd reflns	2266	4601	5870
params	364	481	450
GOF on F^2	1.085	1.042	1.058
R1, wR2 [$I > 2\sigma(I)$]	0.0788, 0.1599	0.0454, 0.1111	0.0501, 0.1118
R1,wR2 (all data)	0.1545, 0.2064	0.0621, 0.1355	0.0608, 0.1225
largest difference peak and hole (e $Å^{-3}$)	0.272, −0.272	0.623, −0.915	0.705, −0.500

owing to its quadrupole carboxyl dentate arms. However, to the best of our knowledge, BPTC transition metal complexes have not been studied so far. With the aim of understanding the coordination chemistry of BPTC and preparing new materials with interesting structural topology and excellent physical properties, we have recently engaged in the research of this kind of polymer complex. We also notice that the introduction of N-containing auxiliary ligands, such as 4,4′-bipyridine, pyrazine, etc., into the {M−BPTC} (M = transition metal) system may lead to new structural evolution and fine-tune the structural motif of these metal−organic hybrid compounds.[5] Herein we report three interesting polymeric complexes with mixed organic ligands, (H_2BPTC)-(4,4′-H_2bpy)H_2O (**1**), [Cd_2Cu(HBPTC)$_2$(μ_2-4,4′-bpy)$_2$(4,4′-bpy)$_2$(H_2O)$_2$]$_n$ (**2**), and [Co_3(HBPTC)$_2$(μ_2-4,4′-bpy)$_3$(H_2O)$_4$]n·2$n$$H_2O$ (**3**). Our results demonstrate that the BPTC ligand can form new building blocks in various coordination modes with metals. These building blocks finally aggregate to generate intriguing supramolecular architectures with auxiliary ligands.

Experimental Section

All the syntheses were performed in poly(tetrafluoroethylene)-lined stainless steel autoclaves under autogenous pressure. Reagents were purchased commercially and were used without further purification. Elemental analyses of C, N, and H were performed on an EA1110 CHNS-0 CE elemental analyzer. IR (KBr pellet) spectra were recorded on a Nicolet Magna 750FT-IR spectrometer. And fluorescent data were collected on an Edinburgh FLS920 TCSPC system. Thermogravimetric measurements were carried out on preweighed samples in a nitrogen stream using a Netzsch STA449C apparatus with a heating rate of 15 °C/min. Variable-temperature magnetic susceptibilities in the temperature range 5−300 K were performed on a model CF-1 superconducting extracting sample magnetometer with the powdered sample kept in the capsule for weighing. All data were corrected for diamagnetism of the ligands estimated from Pascal's constants.

Syntheses of (H_2BPTC)(4,4′-H_2bpy)H_2O (1) and [Cd_2Cu(HBPTC)$_2$(μ_2-4,4′-bpy)$_2$(4,4′-bpy)$_2$(H_2O)$_2$]$_n$ (2). A mixture of $CdCO_3$ (0.17 g, 1.0 mmol) and Cu(NO_3)$_2$·3H_2O (0.12 g, 0.5 mmol) with 3,3′4,4′-benzophenone-tetracarboxylic dianhydride (0.16 g, 0.5 mmol) and 4,4′-bpy (0.08 g, 0.5 mmol) in molar ratio 2:1:1:1 and 10 mL of H_2O was placed in a Parr Teflon-lined stainless steel vessel (25 cm^3), and then the vessel was sealed and heated to 160 °C. The temperature was hold for 3 days, and then the reactant mixture was cooled at a rate of 0.5 °Cmin^{-1} to lead to the formations of yellow crystals of **1** (yield: 53% based on 4,4′-bpy) and blue crystals of **2** (yield: 30% based on 4,4′-bpy) in one pot. Anal. Calcd for complex **1**, $C_{27}H_{20}N_2O_{10}$: C, 60.91; H, 3.79; N, 5.26. Found: C, 60.85; H, 3.66; N, 5.30%. IR (solid KBr pellet, v/cm^{-1}) for complex **1**: 3437 (m), 3101 (m), 1718(m), 1651 (vs), 1497 (m), 1401 (s), 1233 (s), 1066 (m), 1008 (w), 813 (m). Anal. Calcd for complex **2**, $C_{74}H_{48}Cd_2CuN_8O_{20}$: C, 53.56; H, 3.04; N, 6.75. Found: C, 53.60; H, 3.11; N, 6.67%. IR (solid KBr pellet, v/cm^{-1}) for complex **2**: 3434 (s), 3152 (s), 1604(s) 1579 (m), 1489 (w), 1401 (vs), 1297 (w), 1073 (w), 1008 (w), 810 (m), 630 (w).

Synthesis of [Co_3(HBPTC)$_2$(μ_2-4,4′-bpy)$_3$(H_2O)$_4$]$_n$·2$n$$H_2O$ (3). Complex **3** was synthesized in an analogous procedure to **2** except that 0.294 g (1 mmol) of Co(NO_3)$_2$·6H_2O was used instead of $CdCO_3$ and Cu(NO_3)$_2$·3H_2O. The reactant mixture was cooled to lead to the formation of yellow crystals of **1** (yield: 58% based on 4,4′-bpy) and red crystals of **3** (yield: 25% based on 4,4′-bpy) in one pot. Anal. Calcd for $C_{64}H_{50}Co_3N_6O_{24}$: C, 52.51; H, 3.44; N, 5.74. Found: C, 52.54; H, 3.41; N, 5.79%. IR (solid KBr pellet, v/cm^{-1}): 3385 (s), 3134 (vs), 1649 (m), 1607 (m), 1574 (m), 1489

(5) (a) Biradha, K.; Seward, C.; Zaworotko, M. J. *Angew. Chem., Int. Ed.* **1999**, *38*, 492. (b) Lightfoot, P.; Snedden, A. *J. Chem. Soc., Dalton Trans.* **1999**, 3549. (c) Pan, L.; Liu, H. M.; Lei, X. G.; Huang, X. Y.; Olson, D. H.; Turro, N. J.; Li, J. *Angew. Chem., Int. Ed.* **2003**, *42*, 542. (d) Kitaura, R.; Seki, K.; Akiyama, G.; Kitagawa, S. *Angew. Chem., Int. Ed.* **2003**, *42*, 428.

Table 2. Selected Bond Lengths (Å) and Bond Angles (deg) of **2** and **3**

	Complex **2**[a]		
Cd(1)−O(1)#1	2.265(4)	Cd(1)−N(1)	2.388(4)
Cd(1)−N(3)	2.306(4)	Cu(1)−O(4)	1.972(3)
Cd(1)−O(2′)#2	2.307(4)	Cu(1)−O(3)	2.683(4)
Cd(1)−OW1	2.315(4)	Cu(1)−N(2)#4	1.987(4)
Cd(1)−O(3)	2.381(4)		
O(1)#1−Cd(1)−N(3)	99.52(15)	OW1−Cd(1)−O(3)	96.54(15)
N(3)−Cd(1)−O(2′)#2	85.72(15)	O(1)#1−Cd(1)−N(1)	166.08(15)
O(1)#1−Cd(1)−OW1	88.22(15)	N(3)−Cd(1)−N(1)	91.71(16)
N(3)−Cd(1)−OW1	172.03(16)	O(2′)#2−Cd(1)−N(1)	96.15(15)
O(2′)#2−Cd(1)−OW1	91.99(16)	OW1−Cd(1)−N(1)	80.92(16)
O(1)#1−Cd(1)−O(3)	85.90(14)	O(3)−Cd(1)−N(1)	86.71(14)
N(3)−Cd(1)−O(3)	86.03(14)	O(4)−Cu(1)−N(2)#4	87.81(15)
O(2′)#2−Cd(1)−O(3)	171.34(13)	O(4)−Cu(1)−N(2)#5	92.19(15)
	Complex **3**[b]		
Co(1)−O(2W)	2.076(3)	Co(2)−N(4)#2	2.155(3)
Co(1)−O(7)	2.115(3)	Co(2)−N(5)	2.166(4)
Co(1)−N(3)	2.123(4)	Co(3)−O(3W)	2.063(2)
Co(1)−N(2)#2	2.173(3)	Co(3)−O(5)	2.104(2)
Co(2)−O(6)	2.082(3)	Co(3)−N(1)	2.120(5)
Co(2)−O(8)	2.108(4)		
O(2W)−Co(1)−O(7)	90.94(15)	O(8)−Co(2)−N(4)#2	92.09(6)
O(2W)−Co(1)−N(3)	89.52(7)	O(6)−Co(2)−N(5)	87.97(6)
O(7)−Co(1)−N(3)	95.19(6)	O(8)−Co(2)−N(5)	87.91(6)
O(2W)−Co(1)−N(2)#2	90.48(7)	N(4)#2−Co(2)−N(5)	180.000(1)
O(7)−Co(1)−N(2)#2	84.81(6)	O(3W)−Co(3)−O(5)	89.22(11)
O(6)−Co(2)−O(8)	91.77(11)	O(3W)−Co(3)−N(1)	90.48(9)
O(6)−Co(2)−N(4)#2	92.03(6)	O(5)−Co(3)−N(1)	89.52(9)

[a] Symmetry transformations used to generate equivalent atoms: #1 $x-1, y, z$; #2 $x-1, y-1, z$; #3 $-x, -y, -z$; #4 $x-1, y+1, z$; #5 $-x+1, -y-1, -z$. [b] Symmetry transformations used to generate equivalent atoms: #1 $-x, y, -z+{}^1/_2$; #2 $x, y-1, z$.

(w), 1401 (vs), 1300 (w), 1246 (m), 1162 (m), 1130 (m), 1093 (m), 814 (m), 631 (w).

X-ray Structure Analyses. X-ray intensities of complexes **1**−**3** were collected on a Siemens Smart CCD diffractometer equipped with graphite monochromated Mo Kα radiation ($\lambda = 0.71073$ Å) at 293(2) K. Empirical absorption corrections were applied to the data using the SADABS program.[6] The structures were solved by the direct method and refined by the full-matrix least-squares on F^2 using the SHELXTL-97 program.[7] All of the non-hydrogen atoms were refined anisotropically. The H atoms bonded to C atoms and N atoms were positioned geometrically and refined using a riding model [C−H 0.93 Å and $U_{iso}(H) = 1.2U_{eq}(C)$; N−H 0.86 Å and $U_{iso}(H) = 1.2U_{eq}(N)$]. The H atoms bonded to O atoms were located from difference maps and refined isotropically with the O−H distances fixed at 0.82 Å [$U_{iso}(H) = 1.5U_{eq}(O)$]. The structure for **1** has not gotten a satisfying reliability factor ($R = 0.0788$), probably as a result of the presence of pure organic ligands. Crystallographic data and other pertinent information for **1**−**3** are summarized in Table 1. Selected bond lengths and bond angles are listed in Table 2. More details on the crystallographic studies as well as atomic displacement parameters are given as Supporting Information as a CIF file.

Results and Discussion

Synthesis and General Characterization. To design new organic−inorganic hybrid compounds with the multifunctional ligands, hydrothermal synthesis has been proven to be a powerful method. In such a relatively low temperature and under the autogenous pressure, problems of ligand solubility and reactivity are minimized, and appropriate O-donor and N-donor ligands can be selected by the metal centers for efficient molecular building during the crystallization process.[8] The complexes **1**−**3** reported here were simply synthesized under hydrothermal reaction conditions. Interestingly, during both the syntheses of complexes **2** and **3**, we obtained complex **1** as a coproduct with high yield. The formation of complex **1** may arise from the following aspects: (1) It is understandable that 3,3′4,4′-benzophenonetetracarboxylic dianhydride can easily been hydrolyzed to H_4BPTC. H_4BPTC in the synthetic system acts not only as a necessary coordination ligand, but also a pH adjuster of the reaction mixture. (2) 4,4′-Bpy plays an important role in the formation of **1**, probably through acting as a reaction template and deprotonation reagent. When a more stable ligand, pyrazine or 4,4′-trimethylenedipyridine, was used instead of 4,4′-bpy in the same reaction, we did not obtain the corresponding coproducts similar to complex **1**.

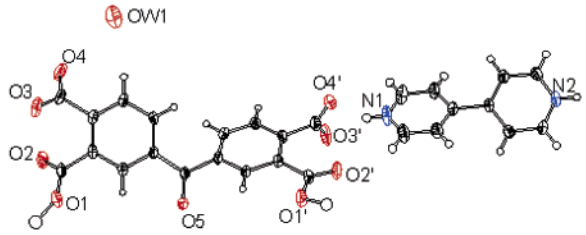

Figure 1. View of **1** with 30% probability displacement ellipsoids. H atoms are shown as small spheres of arbitrary radii.

Table 3. Hydrogen-Bonding Geometry (Å, deg) of Complex **1**

D−H···A	D−H	H···A	D···A	D−H···A
N1−H1B···O3′	0.86	1.85	2.680(6)	161.4
O1−H1A···O3′[ia]	0.84(5)	1.89(3)	2.709(6)	162(6)
N2−H2B···O3[iv]	0.86	1.72	2.580 (5)	176.6
O1′−H1′A···O4[ii]	0.83(5)	1.70(2)	2.524(5)	170(6)
OW1−HW1B···O4	0.84 (2)	2.37 (5)	3.147 (7)	153 (10)
OW1−HW1A···O2[iii]	0.84 (7)	2.24 (9)	2.803 (6)	125 (9)

[a] Symmetry codes: (i) $1-x, 1-y, -z$; (ii) $1+x, {}^1/_2-y, {}^1/_2+z$; (iii) $x, {}^1/_2-y, {}^1/_2+z$; (iv) $1+x, {}^1/_2-y, {}^3/_2+z$.

(H_2BPTC)(4,4′-H_2bpy)H_2O (1). Complex **1** features a 2-D layered hydrogen bonding network with 2-fold interpenetration. As shown in Figure 1, the asymmetric unit contains one H_2BPTC anion, one 4,4′-H_2bpy cation, and one free H_2O molecule. The structure is based on a strong and distinctive pattern of hydrogen bonding interactions (Table 3). Figure 2 shows a 2-D layered hydrogen bonding network and how H_2BPTC units and 4,4′-H_2bpy units are connected to each other through hydrogen bonds. Each H_2BPTC unit links two 4,4′-H_2bpy species through N−H···O hydrogen bonds (N1···O3′ = 2.680 (6) Å and N2···O3[ii] = 2.580 (5) Å) and two other H_2BPTC units through O−H···O hydrogen bonds (O1′···O4[iii] = 2.524(5) Å). These short distances indicate

(6) Sheldrick, G. M. *SADABS*; University of Göttingen: Göttingen, Germany, 1996.
(7) *SHELXTL* (version 5.05); Siemens Analytical X-ray Instruments Inc.: Madison, WI, 1994.
(8) (a) Feng, S. H.; Xu, R. R. *Acc. Chem. Res.* **2001**, *34*, 239. (b) Hagrman, P. J.; Zubieta, J. *Inorg. Chem.* **2000**, *39*, 5218. (c) Hammond, R. P.; Chesnut, D. J.; Zubieta, J. *J. Solid State Chem.* **2001**, *158*, 55. (d) Tao, J.; Zhang, X. M.; Tong, M. L.; Chen, X. M. *J. Chem. Soc., Dalton Trans.* **2001**, 770.

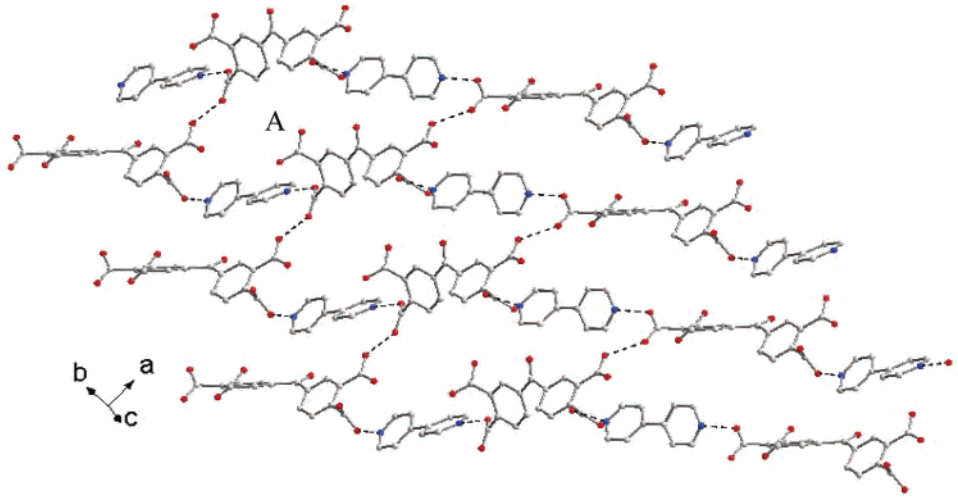

Figure 2. 2-D hydrogen bonding network with a 50-membered large ring A in **1**. The hydrogen bonding interactions are represented by dashed lines.

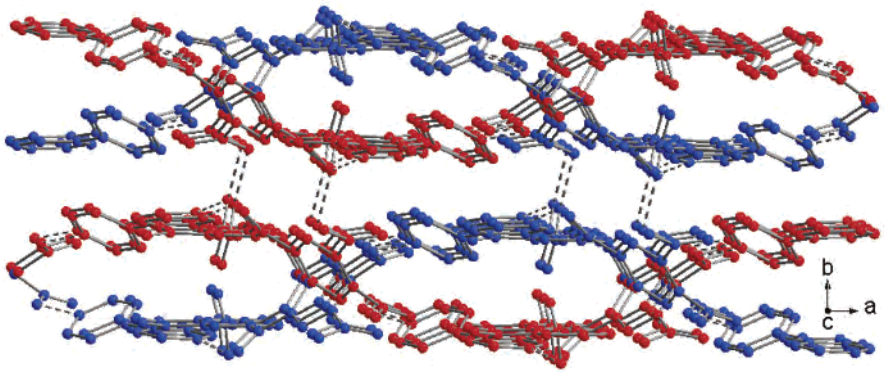

Figure 3. Packing structure along *c*-axis of **1** displaying 2-fold interpenetration. Two 2-D frameworks (red and blue) interpenetrate each other through the large ring A. The hydrogen bonding interactions are represented by dashed lines.

very strong H-bonding interactions. The two phenyl rings from the same H_2BPTC unit twist by 50.55° from each other, and the torsion angles between COO^- group and phenyl ring range from 7.75° to 70.15°. The severely twisted H_2BPTC unit finally results in the wavelike 2-D layer network (Figure 2). There is a 50-membered large ring A in the 2D layer, which is composed of four H_2BPTC and two 4,4′-H_2bpy units. The dimension of the ring A is approximately 6.34 × 22.87 $Å^2$. The void space in the single framework is so large that two 2-D frameworks interpenetrate each other through the large ring as shown in Figure 3. The structure of **1** agrees with the prediction that crystal structures with such large cavities are always stabilized either by inclusion of suitable guests or by interpenetrating lattices. As shown in Figure 3, the adjacent interpenetrated 2D layers are further linked to each other by relatively weaker O−H···O and Ow−H···O hydrogen bonds (d(O1−O3′^{i}) = 2.709(6) Å, d(Ow1−O4) = 3.147(7) Å, and d(Ow1−O2^{iii}) = 2.803(6) Å) to complete the final 3D architecture.

$[Cd_2Cu(HBPTC)_2(\mu_2$-4,4′-bpy$)_2$(4,4′-bpy$)_2(H_2O)_2]_n$ (2). Complex **2** features an unusual two-dimensional double-layered motif with Cu atoms acting as the junctures between the two layers. As shown in Figure 4, the asymmetric unit contains one Cd^{2+} cation, Cu^{2+} cation with an occupancy of 0.5, one HBPTC anion, two 4,4′-bpy molecules, and one H_2O molecule. Each Cd^{II} center has a slightly distorted $\{CdN_2O_4\}$ octahedral coordination sphere and is defined by one nitrogen donor (N1) of a μ_2-4,4′-bpy ligand and one oxygen donor (O1f) of a BPTC ligand in the axial positions. The equatorial positions are occupied by one nitrogen donor of 4,4′-bpy ligand, two oxygen donors from two individual BPTC ligands, and one oxygen from the H_2O molecule. Cd−O bond lengths fall in the range 2.265(4)−2.381(4) Å, and Cd−N bond lengths are 2.388, 2.306 Å, respectively. These values are within the normal experimental limitation (Table 2). The

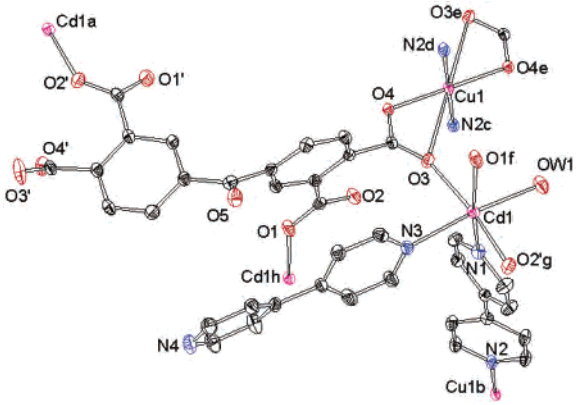

Figure 4. ORTEP drawing of **2** with 30% probability displacement ellipsoids. H atoms and water moleculars were omitted for clarity.

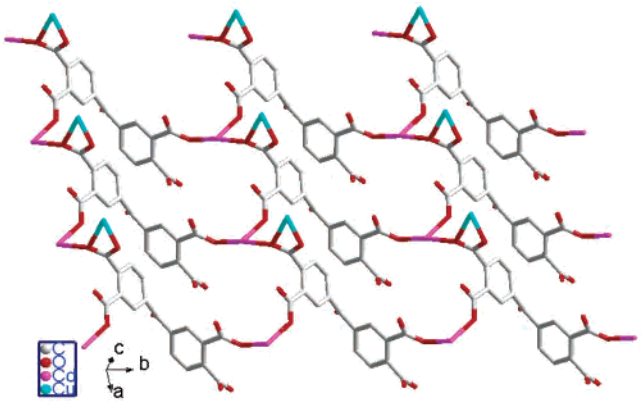

Figure 5. View of Cd atoms interlinked by BPTC ligands to generate a 2-D grid network parallel to (001) in **2**.

Cu^{II} center also has a slightly distorted $\{CuN_2O_4\}$ octahedral coordination sphere, with two nitrogen donors of μ_2-4,4′-bpy ligand in the apical positions (Cu−N = 1.987(4) Å), and four oxygen donors from two carboxylate groups in the equatorial positions (Cu−O = 1.972(3)−2.683(4) Å). These four carboxylate groups on the BPTC anion display different functionality: one group bidentately bridging two different metal centers (Cd^{II} and Cu^{II}) in *anti*−*syn* fashion and two groups monotonically coordinating to two Cd atoms in the *syn* fashion, and the left one does not participate in coordination. The two phenyl rings from the same BPTC unit twist by 79.84° from each other, and the torsion angles between the COO^- group and phenyl ring range from 7.72° to 80.23°. There are two crystallographically independent 4,4′-bpy ligands in their own coordination modes in **2**: one acts as a bidentate bridging ligand binding Cd and Cu simultaneously at the two N ends, the other one acts as a unidentate ligand binding one Cd atom at its one N end while the other N end is involved in hydrogen bond with the uncoordinated carboxylate group of HBPTC ligand (O3′···$N4^i$ = 2.638(6) Å [symmetry code: (i) 2 − *x*, 1 − *y*, −*z*]). As shown in Figure 5, the Cd atoms are interlinked by HBPTC ligands to generate a 2-D layer parallel to (001), which is composed practically of a 32-membered ring. The Cd···Cd distance separations in the layer are 7.525 and 14.137 Å, respectively, and the Cd···Cu distance separated by the bridging carboxylate group is 4.614 Å.

It is interesting to notice that coplanar Cu atoms integrated the adjacent two layers mentioned above in a face-to-face manner into a novel double-layered motif exhibiting large channels (Figure 6) with the approximate dimension 11.46 × 13.47 $Å^2$. A crystallographic C_2 symmetry passes through the center of the channel. μ_2-4,4′-Bpy ligands act not only as μ_2 bridging ligands to support the 2-D framework, but also as guest molecules to fill effectively the nanosized channel (Figure 6). Although several types of double-layered architectures have been fabricated by the assembly of T-shaped[9,10] or rectangular[11] building blocks, this type of molecular double-layered motif is, to the best of our knowledge, unprecedented. The adjacent 2-D bilayers are further linked each other by the O−H···N hydrogen bonds to complete the final 3D architecture (Figure S1).

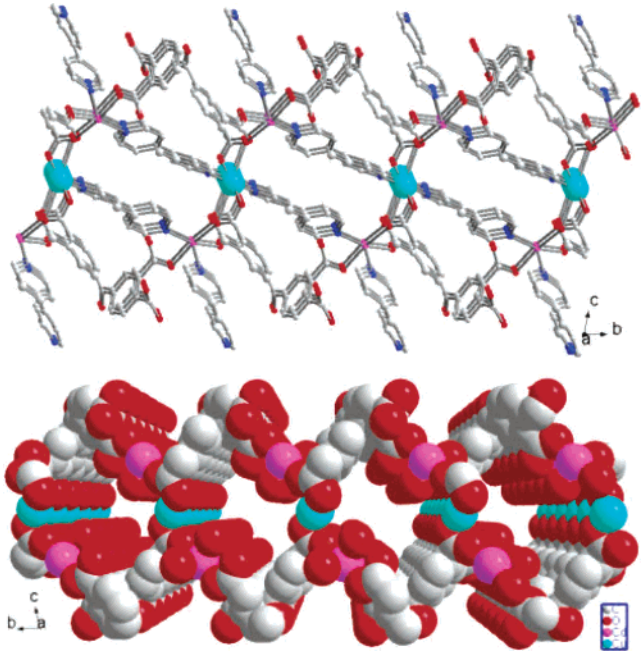

Figure 6. (Top) Molecular double-layered motif displaying nanosized channel filled by 4,4′-bpy bridging ligand in **2**. (Bottom) Space-filling representation of the 1-D nanosized channels with 4,4′-bpy ligands omitted.

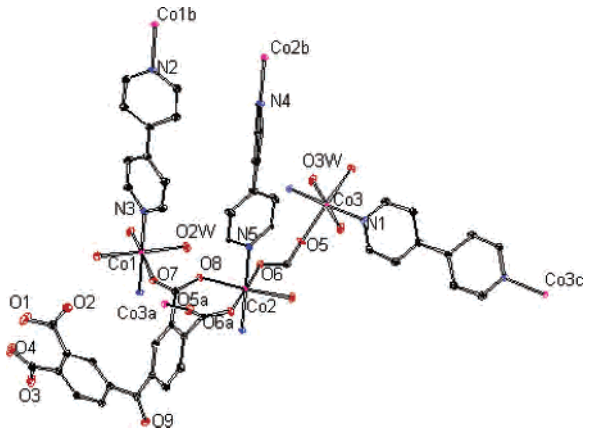

Figure 7. ORTEP drawing of **3** with 30% probability displacement ellipsoids. H atoms and solvent water molecular were omitted for clarity.

$[Co_3(HBPTC)_2(4,4'\text{-bpy})_3(H_2O)_4]_n \cdot 2nH_2O$ (3). Complex **3** features a pillared layer architecture in which the Co(II) ions are integrated by HBPTC ligands into a 2-D wavelike layer network; the layers are further pillared by 4,4′-bpy ligands into a 3-D structure similar to $CdSO_4$. As shown in Figure 7, there are three unique Co(II) atoms in the asymmetric unit. Both Co(1) and Co(3) centers are located on a 2-fold axis and are octahedrally coordinated by two

(9) (a) Power, K. N.; Hennigar, T. L.; Zaworotko, M. J. *New J. Chem.* **1998**, *22*, 177. (b) Dai, J.-C.; Wu, X.-T.; Fu, Z.-Y.; Cui, C.-P.; Hu, S.-M.; Du, W.-X.; Wu, L.-M.; Zhang, H.-H.; Sun, R.-Q. *Inorg Chem.* **2002**, *41*, 1391. (c) Fu, Z.-Y.; Wu, X.-T.; Dai, J.-C.; Hu, S.-M.; Du, W.-X. *New J. Chem.* **2002**, *26*, 978. (d) Kepert, C. J.; Rosseinsky, M. J. *Chem. Commun.* **1999**, 375. (e) Rujiwatra, A.; Kepert, C. J.; Rosseinsky, M. J. *Chem. Commun.***1999**, 2307. (f) Kitagawa, S.; Kondo, M. *Bull. Chem. Soc. Jpn.* **1998**, *71*, 1739. (g) Kondo, M.; Yoshitomi, T.; Seki, K.; Matsuzaka, H.; Kitagawa, S. *Angew. Chem., Int. Ed. Engl.* **1997**, *36*, 1725.
(10) Zaworotko, M. J. *Chem. Commun.* **2001**, 1.
(11) Fu, Z.-Y.; Wu, X.-T.; Dai, J.-C.; Wu, L.-M.; Cui, C.-P.; Hu, S.-M. *Chem. Commun.* **2001**, 1856.

Table 4. Hydrogen-Bonding Geometry (Å, deg) of Complex **3**

D−H···A	D−H	H···A	D···A	D−H···A
O1−H1O···O4	0.839(19)	1.57(2)	2.388(4)	164(6)
O1W−H1WA···O6	0.85(4)	1.95(2)	2.779(5)	165(5)
O1W−H1WB···O3^{ia}	0.86(4)	2.04(2)	2.880(4)	166(5)
O2W−H2WB···O1W	0.797(19)	1.92(2)	2.713(4)	177(4)
O2W−H2WA···O2^{ii}	0.823(19)	1.96(2)	2.771(4)	168(4)
O3W−H3WB···O9^{iii}	0.81(4)	2.01(2)	2.804(4)	167(4)
O3W−H3WA···O3^{i}	0.808(19)	1.94(2)	2.741(5)	171(4)

[a] Symmetry codes: (i) $-x$, $1 + y$, $^1/_2 - z$; (ii) $-x$, y, $^1/_2 - z$; (iii) $1 - x$, $1 + y$, $^1/_2 - z$.

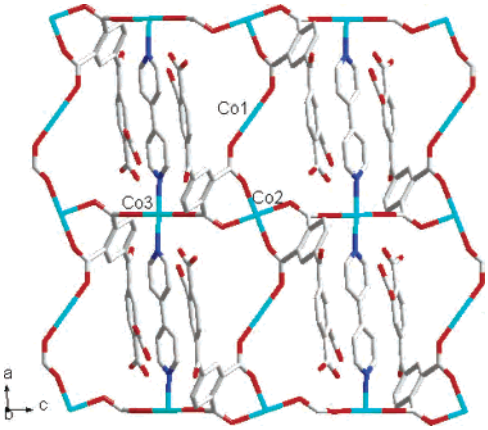

Figure 8. View of the whole Co atoms interlinked by HBPTC ligand to generate a 2D grid layer parallel to (010) in **3**. The coplanar 4,4′-bpy ligands link the symmetric relative Co(3) atoms to form a linear chain.

oxygen donors from two carboxylate ligands, as well as two nitrogen donors from 4,4′-bpy ligands and two aqua ligands. The Co(2) atom, occupying a position of the 2-fold symmetry, is also in an octahedral environment coordinated by four oxygen donors of four carboxylate groups from two individual HBPTC ligands and two nitrogen donors from 4,4′-bpy ligands. The Co−N distances range between 2.120(5) and 2.173(3) Å, and the Co−O bonds range between 2.063(2) and 2.115(3) Å. These distances are comparable to those reported values.[12,13] It is notable that only two carboxylate groups on one side of the HBPTC ligand participate in coordination and both of them are coordinated to Co2 atom. These uncoordinated carboxylate oxygen atoms are involved in hydrogen bonding with aqua ligands and interstitial water molecules (Table 4), increasing the structural stability of the complex. Each coordinated carboxylate group bidentately bridges two Co atoms in *syn*−*anti* fashion, and the torsion angles between the COO^- group and phenyl ring are 78.41° (3 site) and 34.41°(4 site), respectively. All Co atoms are interlinked by the HBPTC ligand to generate a 2-D layer parallel to (010) (Figure 8). The resulting layer is composed practically of 7- and 30-membered rings. The Co···Co separations in this layer are 5.677 (Co2−Co1) and 6.001 (Co2−Co3) Å, respectively. Two symmetric relative Co3 atoms are linked together by coplanar 4,4′-bipyridine, forming a linear chain. As shown in Figure 9, the resulting wavelike layers are strutted by the rigid 4,4′-bipyridine

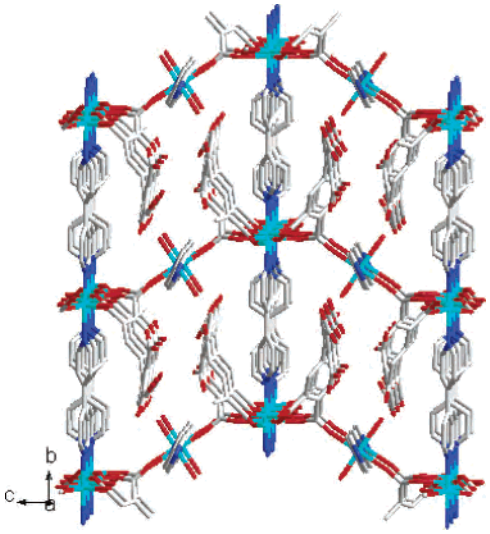

Figure 9. Topology of the structure of complex **3** showing 2-D layers being pillared by rigid 4,4′-bpy ligands.

ligands to form a 3-D open framework exhibiting large tunnel propagating infinitely along the *a*-axis. The tunnel has a diameter of 11.410 × 12.003 $Å^3$ based on the Co···Co distance (between the strutted 4,4′-bipyridine ligand) and the separation between neighboring 4,4′-bipyridine ligands. BPTC ligands are just inside the tunnels. The neighboring 4,4′-bipyridine ligands orient almost perpendicularly to each other so that the side C−H bonds of one 4,4′-bipyridine are directed to the pyridyl plane of the other. The 3-D structural topology of complex **3** is similar to that of $CdSO_4$ (Figure S9).

According to the above structural description of our example compounds, the BPTC ligand exhibits two kinds of bridging modes as shown in Chart 2. In complex **2**, the BPTC ligand bridges three symmetry-related Cd atoms while simultaneously chaleting to a Cu atom, leaving one carboxylate group uncoordinated (Chart 2a). In complex **3**, two adjacent carboxylate groups at one side of the BPTC ligand bridge three different Co atoms while the other two carboxylate groups at the other side are left free (Chart 2b). The assignment of IR spectra of these three complexes revealed its characteristic bands of the asymmetric vibrations between 1718 and 1489 cm^{-1} and the symmetric vibrations at 1401 cm^{-1} (Figure S2).

Thermogravimetric Analyses. To study the stability of the polymers, thermogravimetric analyses (TGA) of complexes **1**−**3** were performed. The TGA diagrams of **1** indicate three main steps of weight losses and support the structural result that there exists a strong hydrogen-bonding network in **1** (Figure S3). The weight loss begins at 126 °C and is completed at 208 °C. The observed weight loss of 3.48% is corresponding to the loss of the crystallization water molecules (calcd 3.38%). The second weight loss occurs in the range 208−292 °C, which can be attributed to the elimination of bpy (calcd 29.32%).[14] The third step is attributed to the further decomposition of BPTC ligands. The

(12) Kuhlman, R.; Schimek, G. L.; Kolis, J. W. *Inorg. Chem.* **1999**, *38*, 194.
(13) Lu, J. Y.; Lawandy, M. A.; Li, J.; Yuen, T.; Lin, C. L. *Inorg. Chem.* **1999**, *38*, 2695.
(14) Song, J. L.; Zhao, H. H.; Mao, J. G.; Dunbar, K. R. *Chem. Mater.* **2004**, *16*, 1884.

Chart 2

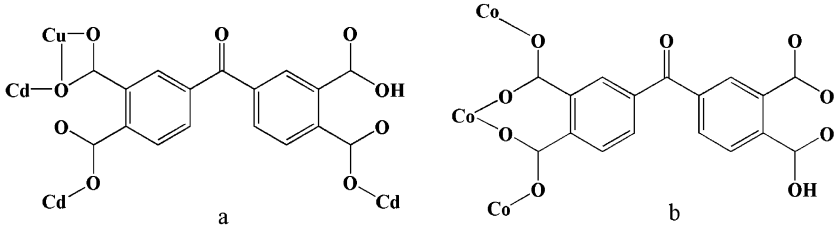

TGA diagrams of **2** indicate two main steps of weight losses (Figure S4). The weight loss begins at 215 °C and is completed at 323 °C. The observed weight loss of 39.71% is corresponding to the loss of the water molecules and bpy ligands (calcd 39.83%). The second step is attributed to the decomposition of the BPTC ligands. The TGA diagrams of **3** indicate three main steps of weight losses (Figure S5). The weight loss begins at 81 °C and is completed at 180 °C. The observed weight loss of 2.48% is corresponding to the loss of the two crystallization water molecules (calcd 2.46%). The second weight loss begins at 190 °C and is completed at 285 °C. The observed weight loss of 37.09% is corresponding to the loss of the four coordinated water molecules and 4,4′-bpy ligands (calcd 36.94%). The third step is attributed to the further decomposition of BPTC ligands.

Photoluminescent Properties. The emission spectra of complexes **1** and **2** in the solid state at room temperature are investigated. It can be observed that an emission occurs at 609 nm (Figure S7, $\lambda_{ex} = 518$ nm) for **1**, which is larger than that of free ligand (3,3′4,4′-benzophenone-tetracarboxylic dianhydride) by a factor of ca. 52 nm, probably due to the H-bonding and the enhanced rigidity of **1**, compared to the free ligand. We tentatively assign it to the intraligand ($\pi-\pi^*$) fluoresence since a weak similar emission with λ_{max} at 557 nm is also observed for the free ligand (Figure S6). The blue fluorescent emission of **1** suggests that it may be used as a new blue-light emitting material. It can also be observed that the intense emissions occurring at 571 nm (Figure S8, $\lambda_{ex} = 460$ nm) for **2**. Interestingly, a clear blue shift of emission occurs in **2**, compared with **1**. Compared to the spectrum of the free ligand, the emission spectrum of complex **2** is neither metal-to-ligand charge transfer (MLCT) nor ligand-to-metal charge transfer (LMCT) in nature. It can be attributed to an intraligand emission state.

Magnetic Property. The temperature-dependent magnetic susceptibility of **3** was measured from 2 to 300 K (Figure S10). The $\chi_m T$ product for this compound is 8.5 $cm^3 \cdot mol^{-1}$ at room temperature and slowly decreases on cooling to a value of 8.4 $cm^3 \cdot mol^{-1}$ at 110 K. However, the curve drops gradually below 110 K, indicating that an antiferromagnetic interaction exists in **3** at lower temperatures. The inverse susceptibility plot as a function of temperature is linear (above 10 K), closely following the Curie−Weiss law with a Curie constant, $C = 8.81$ $cm^3 \cdot mol^{-1} \cdot K$, and a Weiss constant, $\theta = -6.8$ K. The negative θ indicates that there exist predominantly antiferromagnetic interactions in **3**. According to the crystal structure of **3**, it could be presumed that the superexchange interactions between Co(II) ions through the bridging carboxylate groups are weak, which may lead to such magnetic behavior.

Conclusion

Three novel complexes with different architectures, (H_2-BPTC)(4,4′-H_2bpy)H_2O (**1**), [$Cd_2Cu(HBPTC)_2(\mu_2$-4,4′-bpy$)_2$-(4,4′-bpy$)_2(H_2O)_2]_n$ (**2**), and [$Co_3(HBPTC)_2(\mu_2$-4,4′-bpy$)_3$-$(H_2O)_4]_n \cdot 2nH_2O$ (**3**), were constructed from H_4BPTC ligand in the presence of auxiliary 4,4′-bpy ligand. Structural determinations of these complexes in this work have demonstrated that the BPTC ligand has the unique ability to form strong hydrogen bonding network and exhibits remarkable versatility to chelate metals in different coordination modes, forming different interesting topological frameworks. 4,4′-Bpy ligand plays a important role acting as a reaction template and deprotonation reagent. This work also reveals a novel type of 2-fold interpenetrating composite hydrogen bonding network, a new molecular double-layered architecture, and a pillared layer architecture similar to $CdSO_4$ topology.

Acknowledgment. This work was supported by the National Natural Science Foundation of China under Project 20173063, the State Key Basic Research and Development Plan of China (001CB108906), and the NSF of Fujian Province (E0020001).

Supporting Information Available: X-ray crystallographic files in CIF format, figures of IR, TGA curves, photoluminescent spectra. This material is available free of charge via the Internet at http://pubs.acs.org.

IC0491074